Am J Cancer Res 2021;11(10):4826-4843
www.ajcr.us /ISSN:2156-6976/ajcr0133549

Original Article

Identification of potential immune-related circRNA-miRNA-mRNA regulatory network in cutaneous squamous cell carcinoma

Yuanfeng Wei[1*], Xi Yang[1*], Limin Gao[2], Ju Yang[3], Lingnan Zheng[1], Ling Gao[1], Xiaohan Zhou[1], Xiaoyu Xiang[2], Jie Zhang[4], Cheng Yi[1]

[1]Department of Medical Oncology, Cancer Center, West China Hospital, Sichuan University, Chengdu 610041, Sichuan, China; [2]Department of Pathology, West China Hospital, Sichuan University, Chengdu 610041, Sichuan, China; [3]Department of Pathophysiology, West China School of Basic Medical Sciences and Forensic Medicine, Sichuan University, Chengdu 610041, Sichuan, China; [4]Lab of Experimental Oncology, State Key Laboratory of Biotherapy and Cancer Center, West China Hospital, Sichuan University and Collaborative Innovation Center, Chengdu 610041, Sichuan, China. [*]Equal contributors.

Received March 25, 2021; Accepted September 21, 2021; Epub October 15, 2021; Published October 30, 2021

Abstract: Circulating RNAs (circRNAs) are involved in tumor development and progression by participating in immune regulation. Nevertheless, the circRNAs expression profiles and their roles on the immunomodulatory effects in cutaneous squamous cell carcinoma (cSCC) have rarely been studied. In our study, we identified the differentially expressed circRNAs (DEcircRNAs), miRNAs (DEmiRNAs), mRNAs (DEmRNAs) in cSCC and established the circRNA competing endogenous RNAs (ceRNAs) network. Subsequently, the hub differentially expressed immune-related genes were identified and validated by immunochemistry as well as the GO and KEGG pathway analysis were performed. 54 differentially expressed circRNAs were identified and hub differentially expressed immune-related genes were identified and they were mostly associated with immune response in the progression of cSCC. Our results indicated that the potential immune-related circRNA-miRNA-mRNA network may assist in understanding the molecular mechanisms underlying the carcinogenesis and progression in cSCC. Moreover, the immune-related genes may provide an insight into the pathogenesis, molecular biomarkers, and potential therapeutic targets for cSCC patients.

Keywords: Cutaneous squamous cell carcinoma, circRNAs, immune-related genes

Introduction

Cutaneous squamous cell carcinoma (cSCC) is one of the most common non-melanoma skin malignant tumors derived from epidermal keratinocytes, accounting for about 20% of skin tumors, with high metastasis and mortality rates [1, 2]. But due to lack of typical early presentation, most patients in clinical diagnosis often have an aggressive cSCC that usually spreads to other tissues and organs when they were confirmed [3]. Currently, the main treatment options are surgical resection, radiotherapy and chemotherapy. Most patients have better outcomes with surgical resection at an early stage [4]. However, extensive locally destructive or metastatic lesions remain difficult to manage and the prognosis is poor [5, 6]. Therefore, intensive investigation of the regulatory factors involved in cSCC progression is imperative. Meanwhile, more reliable diagnostic and therapeutic biomarkers should be further studied.

Circular RNA, one of endogenous long-stranded non-coding RNAs, formed by reverse splicing in a class of covalently closed single-stranded circular, is widespread in eukaryotic cells [7]. Moreover, it has the characteristics of stability, richness, conservation, localization, and disease-specificity [8, 9]. Notably, it has been revealed that circRNAs play a critically important role in the progression of numerous diseases, such as tumors [10, 11], cardiovascular

diseases [12, 13], metabolic diseases [14] and digestive system diseases [15, 16]. Moreover, the investigators have discovered that circRNAs were rich in miRNA binding sites, which could competitively adsorb miRNAs and influence their functions [17]. Furthermore, a multitude of researches have shown that aberrant circRNA expression played an essential role in cancer through the circRNA-miRNA-mRNA regulatory axis and thereby influence the development and progression of cancer [18-20]. For example, Ma et al. revealed that hsa_circ_0004872 could suppresses gastric cancer progression by competitively binding miR-224/Smad4/ADAR1 pathway [21]. Zhang et al. found that circFGFR1 could sponge miR-381-3p to promote the progression of non-small cell lung cancer (NSCLC) and anti-PD-1 resistance [22]. Nevertheless, the tumor microenvironment is extremely complex, and it is not optimal to focus on one or more relationships of competing endogenous RNAs (ceRNAs) in a single isolated way.

Recently, increasing evidences have pointed that the immune response was involved in the development of cSCC [23, 24]. More importantly, the latest developments suggested that circRNAs were not only engaged in the innate immune responses but also exert their role in tumor immunity [25, 26]. Wei et al. found that circ_0020710 could facilitate the progression and immune evasion of melanoma by the regulation of miR-370-3p/CXCL12 axis [27]. Another study also suggested that circ-CPA4/let-7 miRNA/PD-L1 axis could modulate immune escape in NSCLC [28]. Li et al. discovered that circ_0000284 could contribute to the development of NSCLC by competitively binding miR-377 to upregulate PD-L1 expression [29]. However, previous studies have just concentrated on individual circRNAs, there has been few report regarding the roles of circRNAs acting as a miRNA sponge to impact the immune-related genes of cSCC thereby affecting its progression.

Recognizing the essential of the immune system in malignant cancer, there is an urgency for credible prognosticators and effectively therapeutic targets for cSCC, we identified DEcircRNAs, DEmiRNAs, DEmRNAs and established the circRNA ceRNA network associated with cSCC. From the ceRNA network, we identified immune-related genes and established a PPI network to identify hub immune-related genes to provide new insights for improving clinical diagnosis and potential immunotherapy targets of cSCC patients.

Materials and methods

Data collection and inclusion criteria

We retrieved the microarray data through the GEO database (http://www.ncbi.nlm.nih.gov/geo/). The following search terms were used: 'cSCC' and 'circRNA' or 'miRNA' or 'mRNA'. Moreover, the inclusion criteria of the characteristics of GEO database: (1) the samples including cSCC and normal controls; (2) organism: homo sapiens; (3) experiment type: non-coding RNA profiling or expression profiling were detected by microarray; (4) platforms: circRNA and miRNA were detected by Agilent; mRNA by Affymetrix Human Genome U133 Plus 2.0 Array; (5) sample source: tissue.

Identification of DEcircRNAs and annotation of circRNAs

The DEcircRNAs were identified via limma R package according to the criteria of $|\log_2$ (fold change)| ($|\log_2$ FC|)>2.0 and *P*-value <0.05 after standardization and $\log_2$ transformation of the raw microarray data. Then, we annotated DEcircRNAs using circBase [30]. Moreover, the details information of circRNA were downloaded from circBase. Next, we used the website tools of Cancer-Specific CircRNA (CSCD) to predict their basic structural patterns. Finally, circRNAs' parental genes were used to GO and KEGG pathway analysis by FunRich software (version 3.1.3) and KOBAS, respectively.

Identification of DEmiRNAs and prediction the target miRNAs of circRNAs

The DEmiRNAs were obtained according to $|\log_2$ FC|>2.0 and *P*-value <0.05. Furthermore, "miRNA sponge" is widely considered to be a potential explanation for the work of circRNAs. In order to investigate the miRNAs sponged to DEcircRNAs, the circular RNA Interactome (https://circinteractome.nia.nih.gov/) was used to predict target miRNAs for DEcircRNAs. The above target miRNAs were further filtered by DEmiRNAs based on GE034536, and these target miRNAs and DEmiRNAs were overlapped by Venny 2.1.0 to find the intersection.

Identification of DEmRNAs and prediction of miRNA-mRNA pairs

The differentially expressed mRNAs (DEmRNAs) was screened out with the $|\log_2 FC|>1.0$ and *P*-value <0.05. Moreover, the targeting miRNAs of DEcircRNAs and DEmiRNAs were overlapped as the ultimate miRNAs to further study. Subsequently, the miRNA-mRNA interactions were predicted using miRDB, miRTarBase and TargetScan. Only target mRNAs identified by the three databases were selected for intersection with DEmRNAs to obtain the final functional genes (FmRNAs).

Constructing the circRNA-miRNA-mRNA network

The ceRNA network was constructed with the final circRNAs, miRNAs, and mRNAs, which obtained from the above steps. Visualization of ceRNA network used R software.

GO and KEGG pathway of mRNAs in the network

To assess functional enrichment, FunRich3.1.3 was used to perform GO analysis and KOBAS was adapted to conduct KEGG pathway analysis of final mRNAs (FmRNAs) in the circRNA-miRNA-mRNA network.

Constructing PPI network and identification of hub genes

The PPI network of the DEmRNAs in ceRNAs network was established using the STRING database (http://string-db.org/) with the minimum required interaction score was set to 0.4, and then visualized using Cytoscape 3.7.1 software. The apps in Cytoscape (CytoHubba and MCODE) were used to clarify hub genes and analyze modules, respectively. Then, the expression of some hub genes was confirmed by immunohistochemistry in HPA database and clinical samples.

Immune-related gene set

The lists of immune-related genes were obtained from the ImmPort (https://www.immport.org/shared/home) databases. Then, the differentially expressed immune-related genes were obtained by overlapped with DEmRNAs and the lists of immune-related genes. Then they were analyzed by GO and KEGG analyses to explore their functions. Similarity, the differentially expressed immune-related genes were also used to conduct a PPI network and selected the hub genes and validated by immunohistochemistry in HPA database and clinical samples.

Tissue samples

28 cases of Formalin-fxed, parafn-embedded cSCC tissue and 27 cases of non-cancerous tissue were collected from the Department of Pathology, West China Hospital, Sichuan University from 2018 to 2021. The Ethical Committee of West China Hospital approved this study and waived informed consent.

Immunohistochemistry

The paraffin-embedded tissue sections were used for immunohistochemical staining. Briefly, the tissue sections were deparaffinized and then rehydrated. The second step was antigen retrieval and followed by blocking endogenous peroxidase activity. Next, the primary antibodies were incubated and the main information as follows: anti-ISG15 (1:100 dilution, Cat no#15981-1-AP, Proteintech), anti-RSAD2 (1:200 dilution, Cat no# 28089-1-AP, Proteintech), anti-PI3 (1:200 dilution), anti-OAS3 (1:100 dilution, Cat no#21915-1-AP, Proteintech), anti-CXCL10 (1:200 dilution, Cat no#10-937-1-AP, Proteintech), anti-USP18 (1:1000 dilution, Cat no#GB111923, Servicebio), anti-IL7R (1:100 dilution, Cat no#DF6362, Affinity). The semi-quantitative criterion of evaluating protein levels was based on the intensity of staining and the proportion of positive cells. According to the staining intensity, the results were as follows: 0 (no stain), 1 (light yellow), 2 (brown) and 3 (tan). Additionally, based on the proportion of positive cells, there were five grades: 0 (0%), 1 (1-25%), 2 (26-50%), 3 (51-75%) and 4 (76-100%). The final result was multiplied the two scores. Finally, if the score was more than 6, it was considered high, otherwise the opposite.

Results

Characteristics of eligible GEO database

A total of 13 GEO databases related to keywords were searched. The flow chart diagram of the screening process is shown in **Figure 1**.

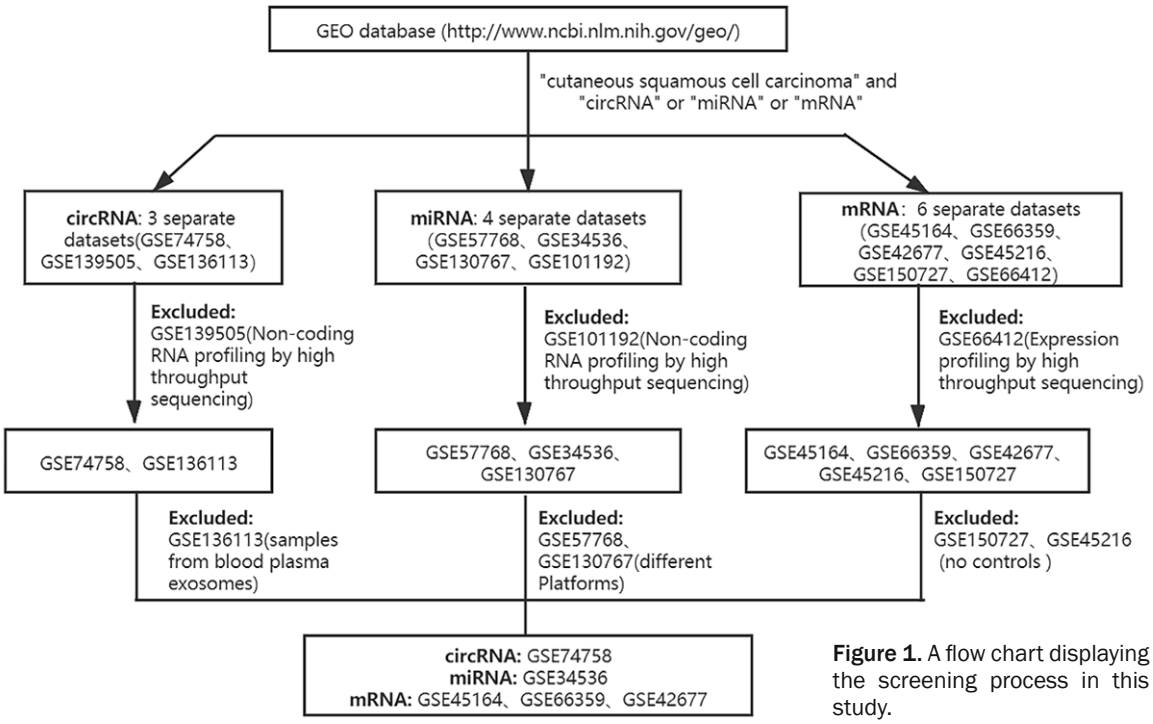

Figure 1. A flow chart displaying the screening process in this study.

Three of them are circRNA databases (GSE74758, GSE139505, GSE136113), four are miRNAs (GSE57768, GSE34536, GSE130767, GSE101192), and six are mRNAs (GSE45164, GSE66359, GSE42677, GSE45216, GSE150727, GSE66412). According to the inclusion criteria, in the end only GSE74758, GSE34536, GSE45164, GSE66359, and GSE42677 met the criteria for inclusion in this study. The following key information was collected from each GEO database: organism, platform, contributor(s), experiment type, last update year, region, sample size, detected RNA, which were listed in Supplementary Table 1.

Identification of differentially expressed circRNAs and annotation of circRNAs

A total of 54 DEcircRNAs were identified by comparing the 3 cSCC and 3 non-lesional skin tissues in the GSE74758 dataset (**Figure 2**). Then, we clarified the detailed information regarding these DEcircRNAs through the circBase database, such as the position, best transcript and gene names (Supplementary Table 2).

Enrichment analysis of circRNAs' parental genes

To explore the functions of DEcircRNAs based on their parental genes in cSCC patients, GO and KEGG analysis were performed. The results showed that the most significant GO terms for biological process (BP) were energy pathways, and metabolism (**Figure 3A**). For cellular component (CC), endoplasmic reticulum membrane, COPII vesicle coat and gamma-tubulin ring complex were the most significant terms (**Figure 3B**). Furthermore, CoA-ligase activity, mannosyltransferase activity, and transporter activity were the most enriched term for molecular function (MF) (**Figure 3C**). Moreover, the enriched pathways analysis by KEGG were most related to mitophagy, renal cell carcinoma, PPAR signaling pathway, prostate cancer, HIF-1, and AMPK signaling pathway (**Figure 3D**).

Predicted the targets miRNAs of circRNAs

To further elucidate the functions of circRNAs, the top 6 up and 6 down-regulated circRNAs were identified as candidate circRNAs to further study according to the |logFC| value, including hsa_circ_0068631, hsa_circ_0070933, hsa_circ_0067772, hsa_circ_0003528, hsa_circ_0070934, hsa_circ_0001955, hsa_circ_0022392, hsa_circ_0022383, hsa_circ_0005085, hsa_circ_0046449, hsa_circ_0072279, and hsa_circ_0000375. Their basic structural patterns were shown in Supplementary Figure 1 based on the data from CSCD. Next, the above most 12 significantly changed

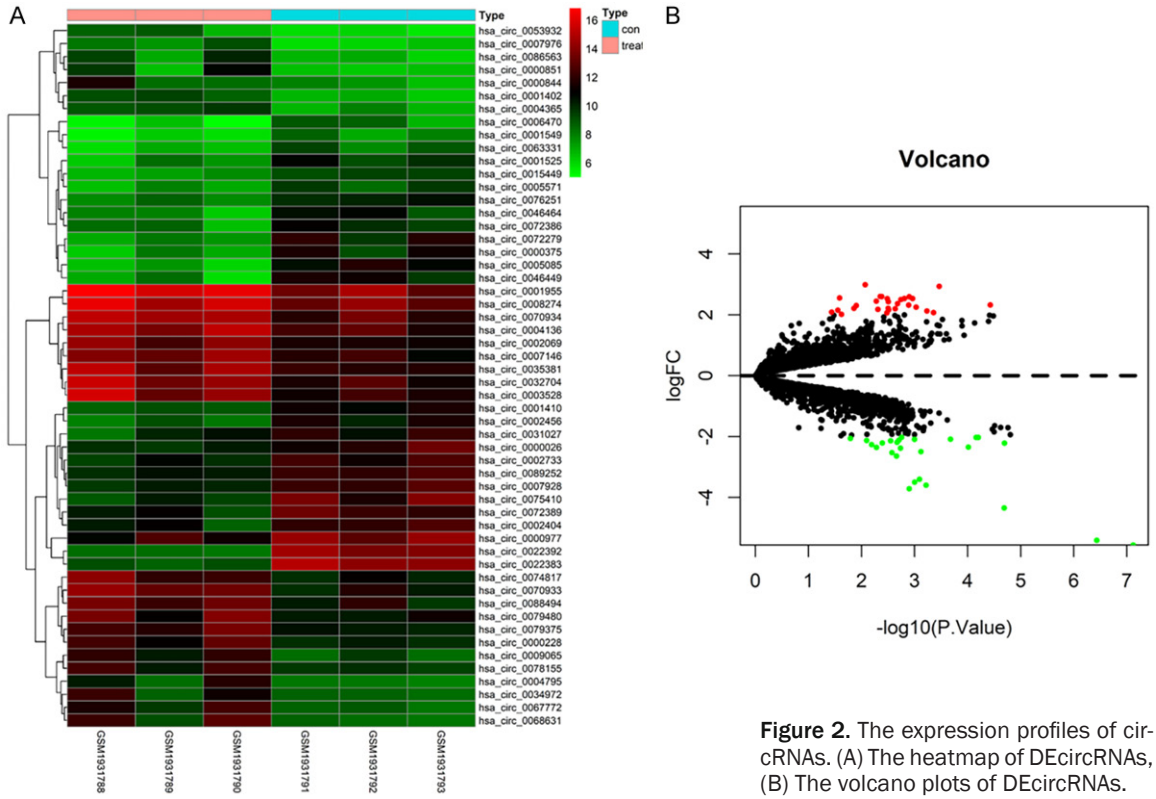

Figure 2. The expression profiles of circRNAs. (A) The heatmap of DEcircRNAs, (B) The volcano plots of DEcircRNAs.

circRNAs were used to predict downstream miRNAs and we identified 215 circRNAs-miRNAs pairs in **Table 1**.

Differential expression of miRNAs in cSCC patients

Based on the GSE34536 database, we obtained 21 DEmiRNAs, including 11 upregulated and 10 down-regulated (**Figure 4A**, **4B**). Then, intersection of miRNAs predicted by 12 top circRNAs and DEmiRNAs. Finally, two miRNAs of hsa-miR-136 and hsa-miR-766 were obtained as candidate miRNAs (**Figure 4C**).

Differential expression of mRNAs in patients with cSCC and the targets of miRNAs

After comparing the 10 tumor tissues and 3 normal tissues in the GSE45164 database, we filtered and obtained 974 DEmRNAs, which were made up of 502 up-regulated and 472 down-regulated genes (**Figure 4D**). Meanwhile, 1252 DEmRNAs were selected in the GSE66359 dataset, including 656 up and 596 down-regulated genes (**Figure 4E**). Moreover, 2888 DEmRNAs were identified in the same way from the GSE42677 dataset, and it included 1432 up-regulated and 1456 down-regulated genes (**Figure 4F**). The number of common genes in both three GEO database was 66 genes (**Figure 4G**). There were 129 target genes of predicted miRNAs through miRDB, miRTarBase, and TargetScan databases (**Figure 4H**). Finally, 36 common genes (FmRNAs) were obtained by interact 129 target genes of predicted miRNAs and 66 genes among three GEO databases (**Figure 4I**).

The circRNA-microRNA-mRNA interaction network

Increasing evidence has suggested that circRNAs may play a role in regulating the functions of target mRNAs as miRNA sponges. In order to further make sense the potential roles of the DEcircRNAs in cSCC, the circRNA-microRNA-mRNA interaction network was constructed. Among the top 12 DEcircRNAs, the predicted miRNAs of six circRNAs were not found in the DEmiRNAs, so only 6 circRNAs, 2 miRNAs and 36 target mRNAs were used to construct the network (**Figure 5A**). We found that hsa-miR-136 was predicted to be common downstream of hsa_circ_0070933, hsa_circ_0022392 and hsa_circ_0070934, which indicated that there might be some functional connection between them. These RNA interactions

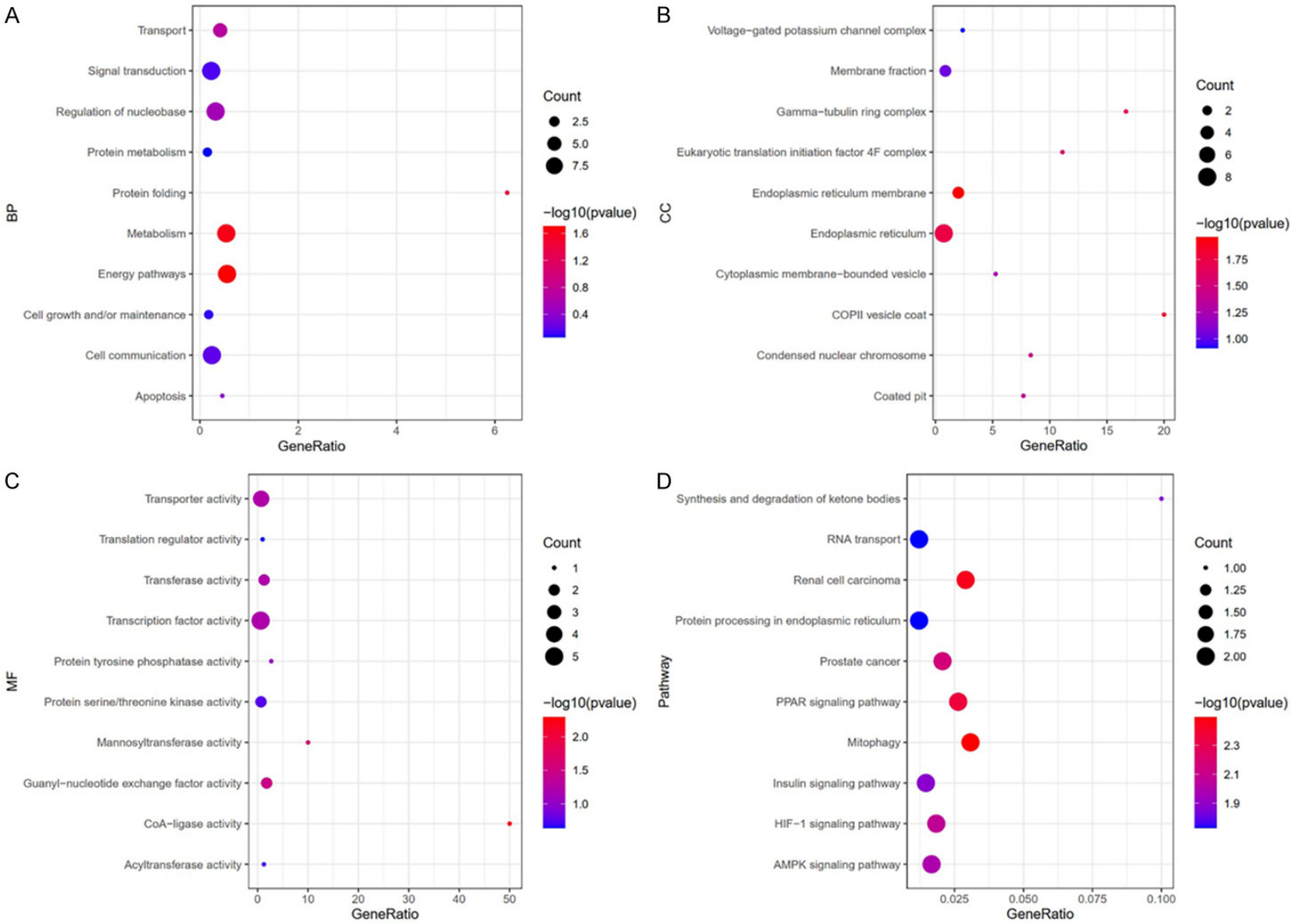

Figure 3. Top 10 Gene Ontology terms and Kyoto Encyclopedia of Genes and Genomes (KEGG) pathway enrichment analysis of 54 differentially expressed circRNAs' parental genes. A-C. The biological process, cellular component and molecular function of GO terms, respectively. D. KEGG pathway enrichment analysis of the genes.

Table 1. The target miRNAs of DEcircRNAs

CircRNA	Position	Target microRNA number	Target microRNA
hsa_circ_0068631	chr3:195802029-195803993	8	hsa-miR-1303, hsa-miR-139-5p, hsa-miR-515-5p, hsa-miR-599, hsa-miR-615-3p, hsa-miR-640, hsa-miR-659, hsa-miR-758
hsa_circ_0070933	chr4:128995614-128996148	7	hsa-miR-1290, hsa-miR-1304, hsa-miR-136, hsa-miR-1825, hsa-miR-431, hsa-miR-515-5p, hsa-miR-526b
hsa_circ_0067772	chr3:155547476-155560408	26	hsa-miR-1183, hsa-miR-1225-5p, hsa-miR-1238, hsa-miR-1256, hsa-miR-1276, hsa-miR-1283, hsa-miR-1286, hsa-miR-1289, hsa-miR-1294, hsa-miR-409-3p, hsa-miR-421, hsa-miR-488, hsa-miR-492, hsa-miR-494, hsa-miR-512-5p, hsa-miR-518a-5p, hsa-miR-527, hsa-miR-548c-3p, hsa-miR-567, hsa-miR-581, hsa-miR-623, hsa-miR-646, hsa-miR-649, hsa-miR-651, hsa-miR-1827, hsa-miR-892a
hsa_circ_0003528	chr5:134032815-134044578	26	hsa-miR-1236, hsa-miR-1248, hsa-miR-1252, hsa-miR-1253, hsa-miR-1279, hsa-miR-1287, hsa-miR-1288, hsa-miR-192, hsa-miR-215, hsa-miR-217, hsa-miR-223, hsa-miR-224, hsa-miR-324-5p, hsa-miR-330-3p, hsa-miR-370, hsa-miR-421, hsa-miR-488, hsa-miR-495, hsa-miR-548, hsa-miR-574-5p, hsa-miR-587, hsa-miR-606, hsa-miR-668, hsa-miR-890, hsa-miR-891b, hsa-miR-892b
hsa_circ_0070934	chr4:128995614-129012667	33	hsa-miR-1208, hsa-miR-1229, hsa-miR-1234,hsa-miR-1236,hsa-miR-1238, hsa-miR-1247, hsa-miR-1263, hsa-miR-1290, hsa-miR-1304, hsa-miR-1305, hsa-miR-136, hsa-miR-1825, hsa-miR-197, hsa-miR-203, hsa-miR-383, hsa-miR-431, hsa-miR-487a, hsa-miR-502-5p, hsa-miR-515-5p, hsa-miR-520g, hsa-miR-520h, hsa-miR-526b, hsa-miR-556-3p, hsa-miR-558, hsa-miR-578, hsa-miR-598, hsa-miR-600, hsa-miR-626, hsa-miR-636, hsa-miR-647, hsa-miR-668, hsa-miR-889, hsa-miR-942
hsa_circ_0001955	chr15:64495280-64508912	32	hsa-miR-1229, hsa-miR-1243, hsa-miR-1252, hsa-miR-1256, hsa-miR-1287, hsa-miR-1296, hsa-miR-1299, hsa-miR-1305, hsa-miR-145, hsa-miR-149, hsa-miR-188-3p, hsa-miR-326, hsa-miR-330-5p, hsa-miR-338-3p, hsa-miR-496, hsa-miR-502-5p, hsa-miR-516a-5p, hsa-miR-520g, hsa-miR-520h, hsa-miR-532-3p, hsa-miR-568, hsa-miR-583, hsa-miR-599, hsa-miR-607, hsa-miR-630, hsa-miR-644, hsa-miR-646, hsa-miR-659, hsa-miR-766, hsa-miR-767-5p, hsa-miR-769-5p, hsa-miR-873
hsa_circ_0022392	chr11:61630443-61631258	8	hsa-miR-1288, hsa-miR-1299, hsa-miR-136, hsa-miR-548b-3p, hsa-miR-657, hsa-miR-665, hsa-miR-766, hsa-miR-873
hsa_circ_0022383	chr11:61605249-61615756	17	hsa-miR-1206, hsa-miR-1245, hsa-miR-1258, hsa-miR-1287, hsa-miR-1324, hsa-miR-197, hsa-miR-495, hsa-miR-498, hsa-miR-524-3p, hsa-miR-525-3p, hsa-miR-624, hsa-miR-629, hsa-miR-635, hsa-miR-665, hsa-miR-766, hsa-miR-7, hsa-miR-876-3p
hsa_circ_0005085	chr2:9419445-9437574	11	hsa-miR-186, hsa-miR-515-5p, hsa-miR-521, hsa-miR-548b-3p, hsa-miR-579, hsa-miR-589, hsa-miR-609, hsa-miR-626, hsa-miR-661, hsa-miR-766, hsa-miR-873
hsa_circ_0046449	chr17:80714040-80758872	32	hsa-miR-1182, hsa-miR-1184, hsa-miR-1205, hsa-miR-1277, hsa-miR-1247, hsa-miR-1299, hsa-miR-186, hsa-miR-361-3p, hsa-miR-433, hsa-miR-450b-3p, hsa-miR-769-3p, hsa-miR-512b-5p, hsa-miR-517a, hsa-miR-517c, hsa-miR-548c-3p, hsa-miR-548p, hsa-miR-587, hsa-miR-1270, hsa-miR-620, hsa-miR-624, hsa-miR-636, hsa-miR-639, hsa-miR-646, hsa-miR-654-3p, hsa-miR-665, hsa-miR-668, hsa-miR-758, hsa-miR-873, hsa-miR-885-3p, hsa-miR-885-5p, hsa-miR-891b, hsa-miR-940
hsa_circ_0072279	chr5:37352838-37358253	7	hsa-miR-139-5p, hsa-miR-488, hsa-miR-518a-5p, hsa-miR-527, hsa-miR-654-3p, hsa-miR-665, hsa-miR-934
hsa_circ_0000375	chr12:6657590-6657991	8	hsa-miR-1182, hsa-miR-1184, hsa-miR-1205, hsa-miR-296-5p, hsa-miR-330-3p, hsa-miR-487a, hsa-miR-490-5p, hsa-miR-622

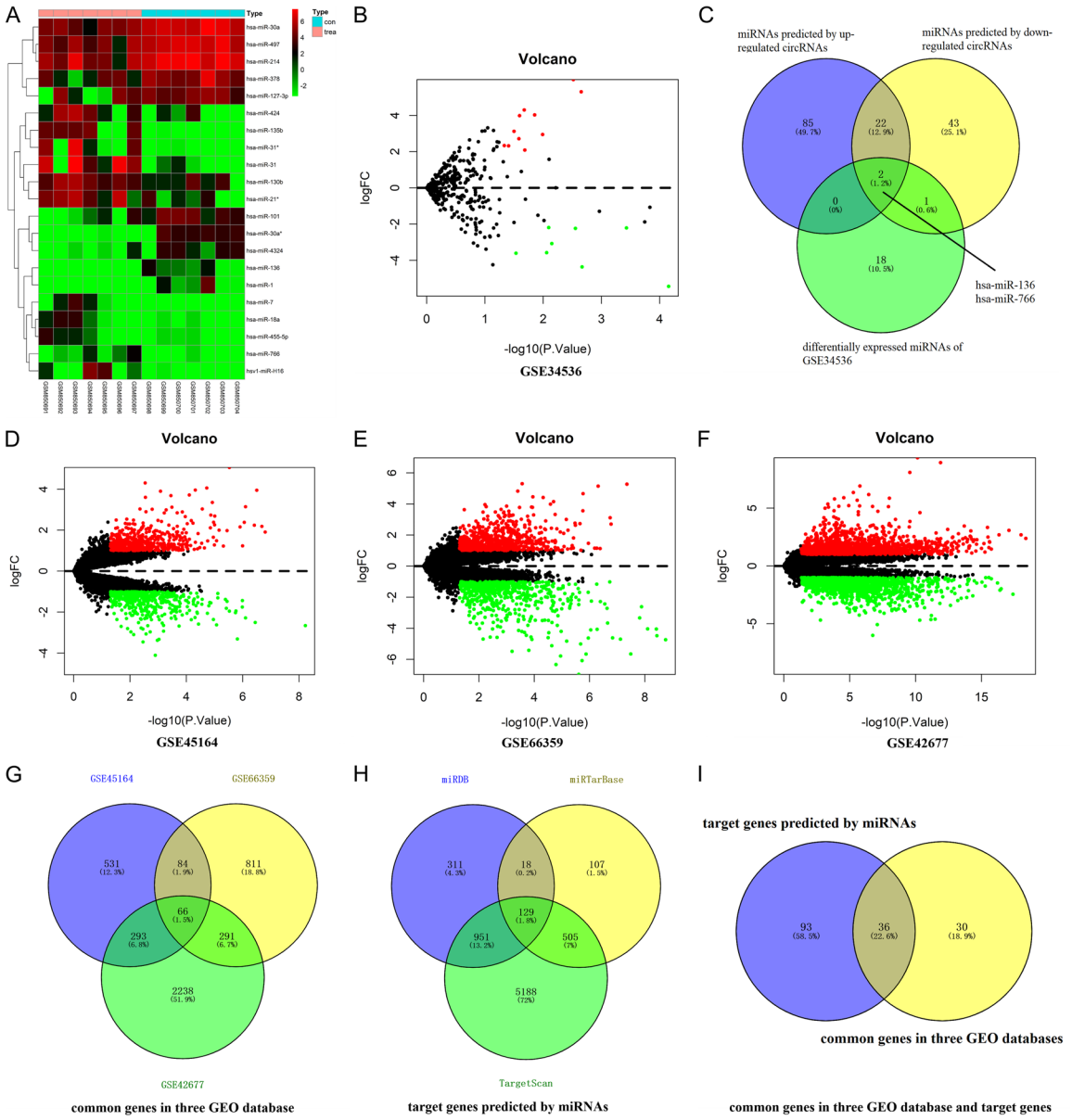

Figure 4. The expression profiles of miRNAs and mRNAs. (A) the heatmap of DEmiRNAs, (B) The volcano plots of DEmiRNAs, (C) intersection of miRNAs predicted by 12 top circRNAs and DEmiRNAs, (D) DEmRNAs in GSE45164, (E) DEmRNAs in GSE66359, (F) DEmRNAs in GSE42677, (G) Common DEmRNAs in both three GEO database, (H) target genes of predicted miRNAs by miRDB, miRTarBase, and TargetScan databases, (I) common genes were obtained by interact 129 target genes of predicted miRNAs and 66 genes among three GEO databases.

may provide new insight into the mechanism underlying cSCC.

Enrichment analysis of the genes in the network

The 36 genes in the network were used to evaluate the biological roles of the circRNAs. The top 10 GO terms of each group are shown in **Figure 5B-D**. In the BP category, the main enriched categories were immune response, spindle assembly and cell growth and/or maintenance (**Figure 5B**). In CC, extracellular, membrane raft, and plasma membrane were the main enriched terms (**Figure 5C**). In MF, the mostly enriched terms were cell adhesion molecule activity, protease inhibitor activity, ATP binding, and deaminase activity (**Figure 5D**). Furthermore, the most enriched KEGG pathways were epstein-barr virus infection, human papillomavirus infection, hepatitis C, influenza

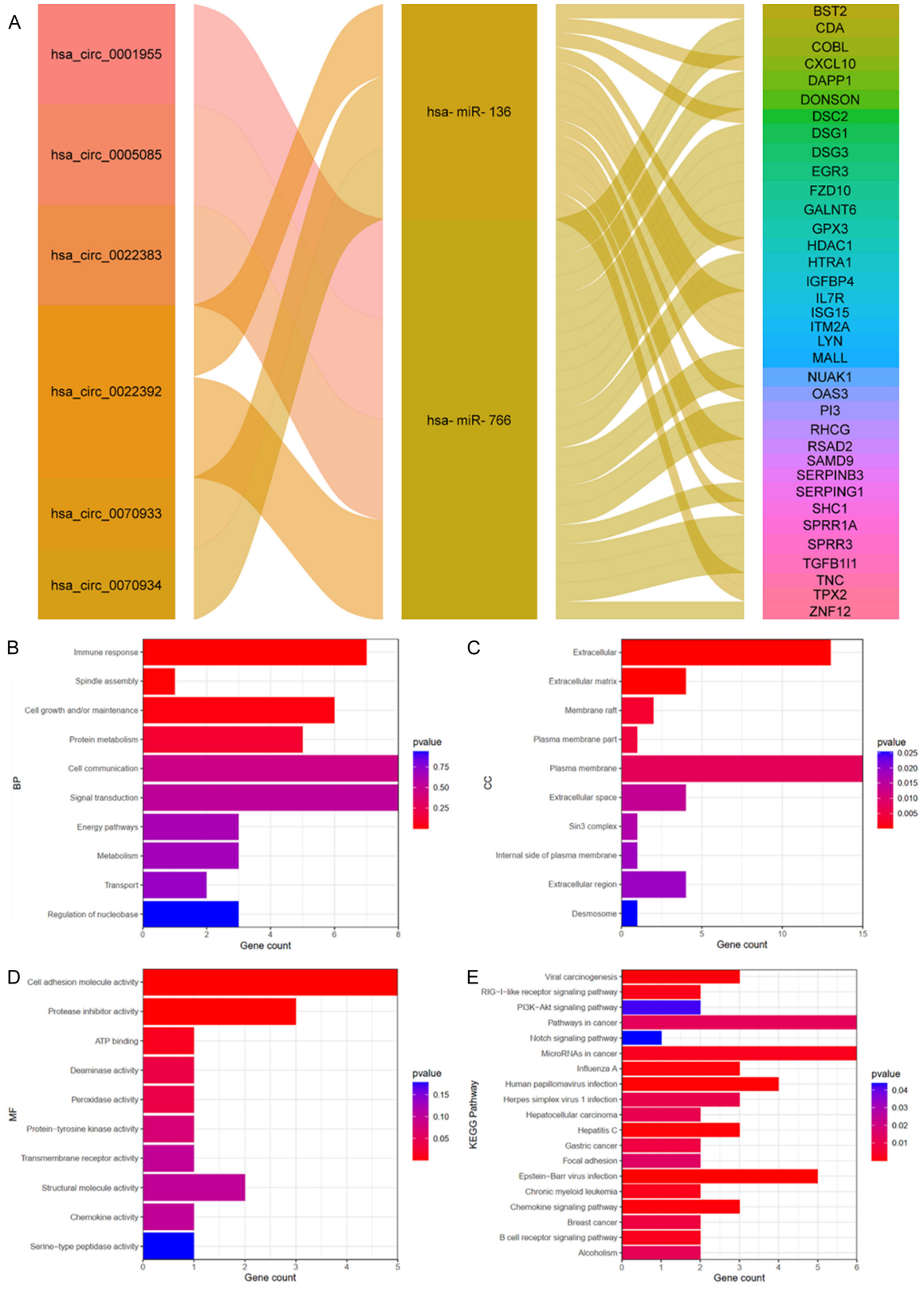

Figure 5. ceRNA network and GO and KEGG pathway analysis of the genes in ceRNA network. (A) ceRNA network, (B) GO terms of BP category, (C) CC category, (D) MF category, and (E) The significant enriched KEGG pathways.

A, chemokine signaling pathway, RIG-I-like receptor signaling pathway, and microRNAs in cancer. The **Figure 5E** showed the most enriched cancer-related pathways.

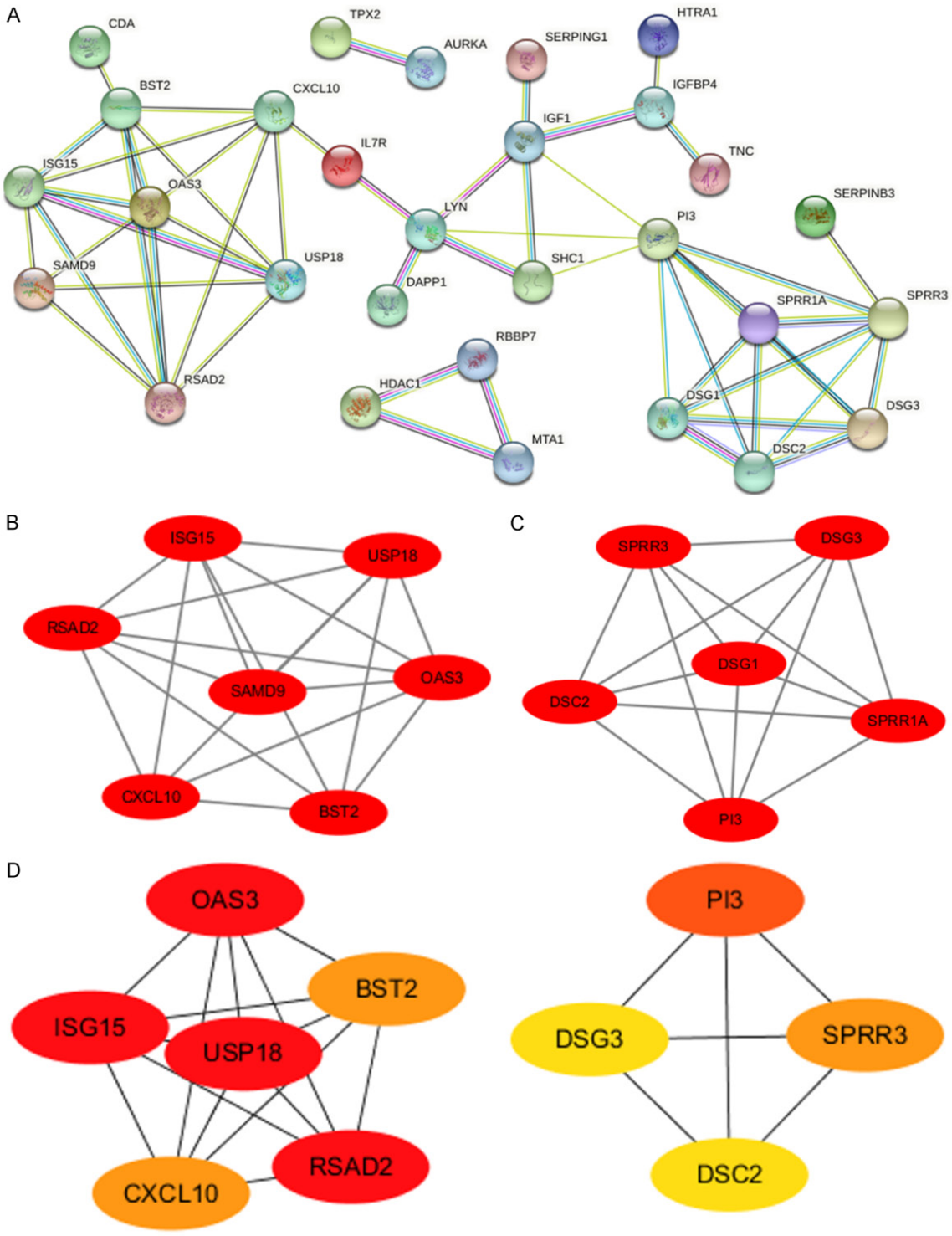

Figure 6. PPI analysis. A. PPI network of 36 genes was constructed in STRING database. B. Module 1 of the PPI network. C. Module 2 of the PPI network. D. Top 10 hub genes selected by the CytoHubba.

Identification of hub genes in the PPI network

According to STRING database, we established a PPI network to show the interactions of the 36 target genes (**Figure 6A**). MCODE in Cytoscape was applied to identify hub module. Two modules were identified, Module 1 consisted of 7 genes and 19 edges (**Figure 6B**), while

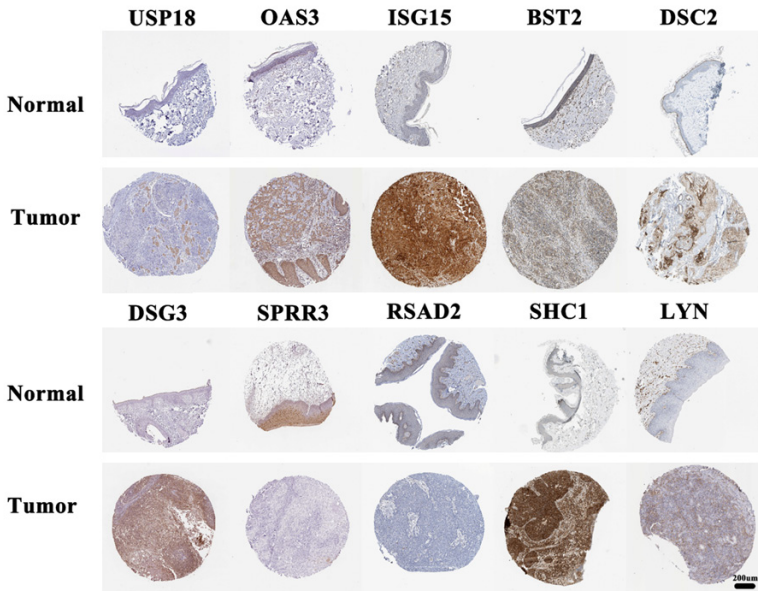

Figure 7. Validation of hub genes by immunohistochemistry in HPA databases. The scale bars represent 200 μm.

module 2 consisted of 6 genes and 15 edges (**Figure 6C**). According to cytoHubba plugin's MCC ranking, the top 10 hub genes were USP18, OAS3, ISG15, RSAD2, PI3, CXCL10, BST2, SPRR3, DSC2 and DSG3, which was shown in **Figure 6D**. Immunohistochemical assays from the HPA database was implemented to conforme the expression of proteins encoded by these hub genes, the result was presented in **Figure 7**. However, PI3 and CXCL-10 protein expression was not found in HPA database. In order to better reveal the reality of our results, we have collected 28 cases of cSCC tissue and 27 cases of non-cancerous tissue from our hospital to validate the top hub gens and the genes that were not found in HPA database (PI3 and CXCL10), the results showed the expression level of USP18 was expressed higher (17/28, 60.7%) than that in controls (9/27, 33.3%). OAS3 was elevated in tumor tissue (19/28, 67.9%) compared with non-cancerous tissue (10/27, 37.0%). Similarly, ISG15 was expressed higher in cSCC (18/28, 64.3%) than controls (10/27, 37.0%). CXCL10 was also up-regulated in tumor tissue (13/28, 46.4%) compared with controls (5/27, 18.5%). Conversely, RASD2 was expressed higher in non-cancerous tissue (12/27, 44.4%) than tumor tissues (5/28, 17.9%). PI3 was expressed lower in tumor (9/28, 32.1%) than controls (15/27, 55.6%). The above results were presented in **Figure 8**.

Identification of immune-related genes and enrichment analysis

10 immune-related differentially expressed genes were obtained by overlapped with selected DEmRNAs in the ceRNA network (FmRNAs) and the lists of immune-related genes (**Figure 9A** and Supplementary Table 3). Next, the PPI network was constructed based on immune-related differentially expressed genes and shown in **Figure 9B**. According to cytoHubba plugin's MCC ranking, the top hub genes were CXCL10, BST2, ISG15, RSAD2, LYN, SHC1, PI3, IL7R, which was shown in **Figure 9C**. CXCL10, BST2, ISG15, RSAD2 and PI3 have been verified above. The expression level of SHC1 and LYN was validated by immunohistochemical assays from the HPA database, the result showed that they were expressed higher in tumor than in controls (**Figure 7**). However, IL7R protein expression was not found in HPA database, our own clinical samples were collected to validate it, the result found that IL7R was expressed higher in tumor (15/28, 53.6%) than in controls (7/27, 25.9%) and presented in **Figure 8**. The GO enrichment analysis of different expressed immune-related genes was carried out to further clarify the biological functions. The genes closely related to the BP terms were immune response and cell communication (**Figure 9D**). Moreover, extracellular, plasma membrane part, and sin3 complex were enriched in CC (**Figure 9E**). Additionally, protein-tyrosine kinase activity, cytokine activity and chemokine activity were mostly enriched in MF terms (**Figure 9F**). Furthermore, KEGG pathway enrichment analysis was significant enriched in RIG-I-like receptor, chemokine signaling pathway, microRNAs in cancer and chronic myeloid leukemia (**Figure 9G**).

Discussion

circRNAs are a cluster of long-stranded non-coding RNAs with a highly stable and conserved structure [31]. Acting as microRNA (miRNA) sponge, it can inhibit miRNA function and regu-

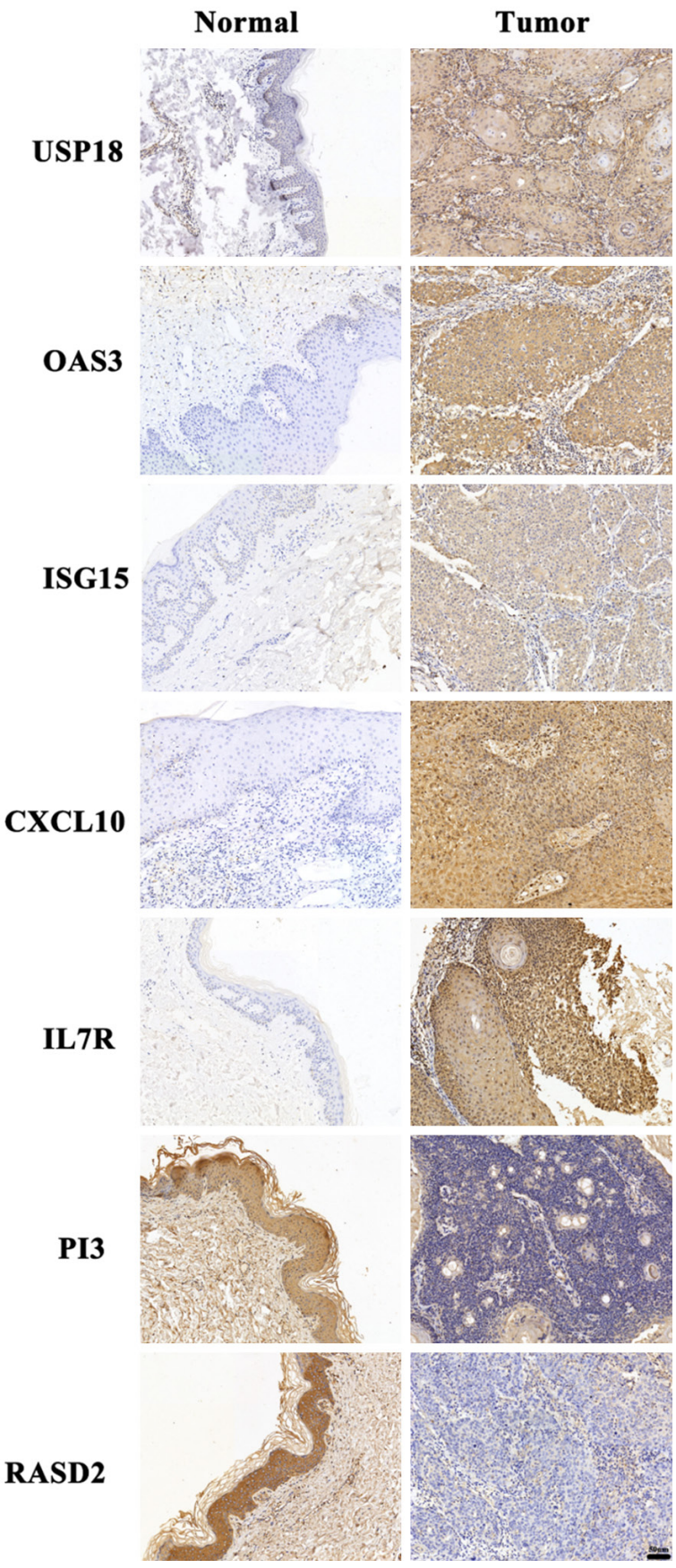

Figure 8. The clinical samples were performed to confirm the protein expression of USP18, OAS3, ISG15, CXCL10, IL7R, PI3, and RSAD2 by immunohistochemistry. The scale bars represent 50 μm.

late its downstream target genes expression in a variety of cancers [10, 32]. In addition, a bunch of studies have suggested that circRNAs could be found commonly expressed in tumor tissues and engaged in the regulation of cancer-related pathways [33, 34]. While there has been just a small number of studies so far exploring the specific role of circRNAs in cSCC [35, 36]. In this study, we identified 54 differentially expressed circRNAs in cSCC and found that their parental genes were most enriched in mitophagy, PPAR, HIF-1, and AMPK signaling pathway. Zhou et al. found that HOXA9 could inhibit the HIF-1α-mediated glycolytic pathway by interacting with CRIP2 to suppress the development of cSCC [37]. An et al. reveled that HIF-1α overexpression might play an crucial role in the occurrence of cSCC [38]. The above results suggested that the parental genes of DEcircRNAs might exert a significant role cSCC progression. However, there are little studies about cSCC and PPAR, AMPK signaling pathway. It is deserved further studied.

The hsa_circ_0070934 was up-regulated in cSCC of 54 differentially expressed circRNAs. Zhang et al. found that the circ_0070934 expression was higher in various cSCC cell lines than in normal human keratinocyte cell lines [39]. This result was similar to a previous study, which has revealed that circ_0070934 was

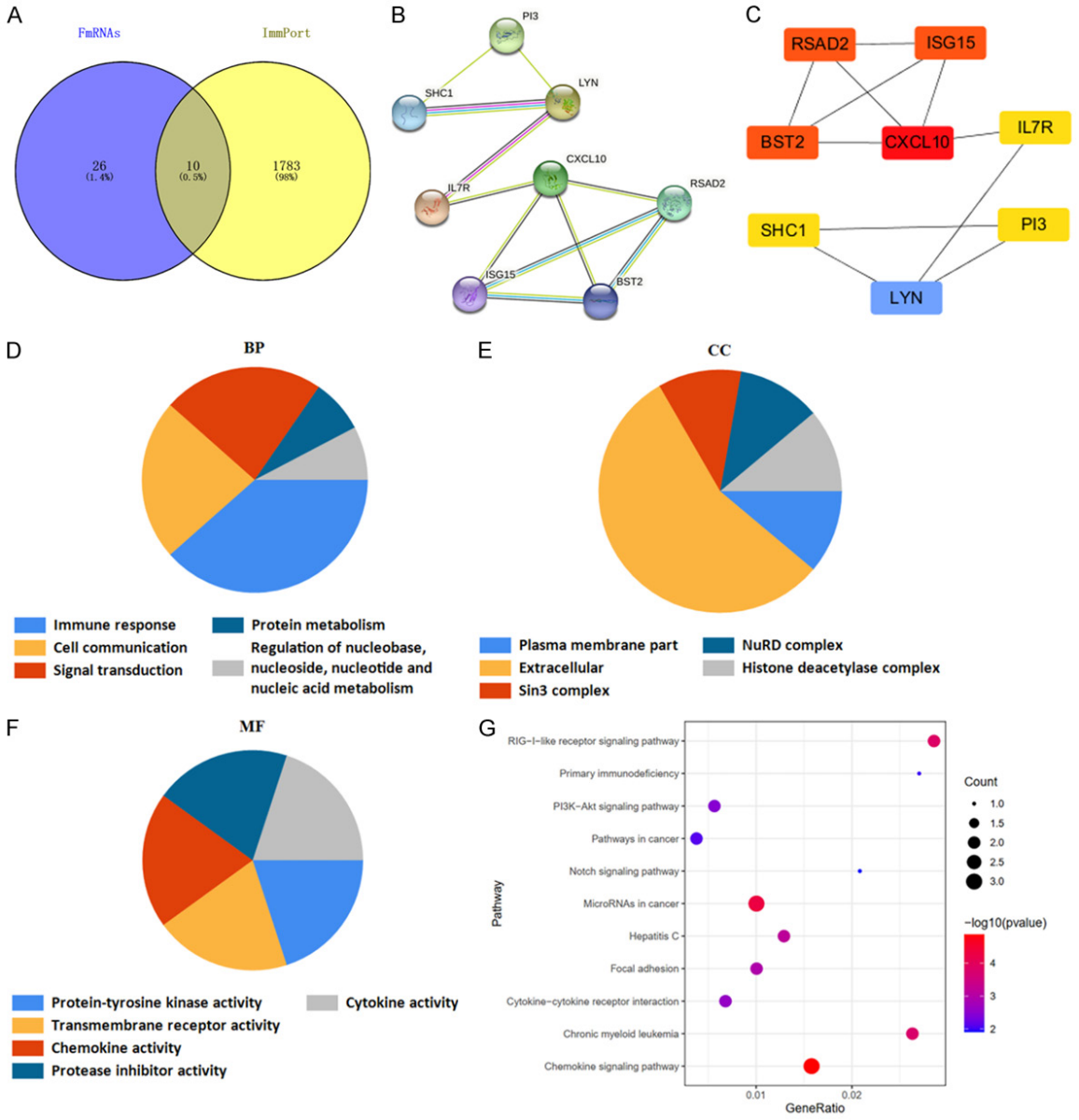

Figure 9. Identification of differentially expressed immune-related genes, constructed PPI network and GO enrichment analysis and KEGG pathway analysis. (A) Identification of differentially expressed immune-related genes, (B) PPI network of 10 genes was constructed in STRING database, (C) top 8 hub genes selected by the CytoHubba, (D) GO terms of BP category, (E) CC category, and (F) MF category, and (G) the significant enriched KEGG pathways.

expressed higher in the cSCC samples compared to the corresponding control samples [35]. An et al. also found that circ_0070934 was overexpressed in cSCC tissue and cell lines [36]. The above results suggested that circ_0070934 might serve as an early diagnostic biomarker of cSCC. Moreover, hsa_circ_0001955, hsa_circ_0070933, hsa_circ_0067772, and hsa_circ_0003528 were found up-regulated in cSCC. while hsa_circ_0022392, hsa_circ_0022383, hsa_circ_0005085, hsa_circ_0046449, hsa_circ_0072279, and hsa_circ_0000375 were most down-regulated, which was consistent with our source data research [35]. Moreover, zhang et al. found that hsa_circ_0001955 was expressed higher in hepatocellular carcinoma [40]. Ding et al. confirmed that hsa_circ_0001955 expression was largely increased in HCC cells and tissues than in corresponding normal controls [41]. Ding et al. identified that hsa_circ_0001955 was significantly up-regulated in colorectal cancer

[42]. However, there was no relevant research in cSCC about it. Moreover, the other top differently expressed circRNAs in cSCC were little known about their expression and function. Further researches shall be implemented to elucidate the underlying mechanisms concerned.

MiRNAs belong to small RNAs and are 20 nucleotides in length. Its main function is to regulate the expression of mRNAs, and thereby regulating cell proliferation, apoptosis, and migration, and thus promoting tumor development [43, 44]. Moreover, some researchers have found that circRNAs could competitively bind to miRNAs and regulate tumor progression [15, 45]. Hao et al. reported that circ_0007534 could promote pancreatic ductal carcinoma progression through binding miR-892b and miR-625 [46]. Niu et al. showed that hsa_circ_0001829 could facilitate gastric cancer development via the miR-155-5p/SMAD2 axis [47]. To elucidate the complex mechanism of circRNAs, we predicted their target miRNAs and identified DEmiRNAs in cSCC patients. We obtained 21 differentially expressed miRNAs, including 11 up-regulated (hsa-miR-135b, hsa-miR-31, hsa-miR-130b, hsa-miR-21*, hsa-miR-766, hsa-miR-31*, hsa-miR-424, hsa-miR-18a, miR-H16, hsa-miR-455-5p, hsa-miR-7) and 10 down-regulated miRNAs (hsa-miR-30a*, hsa-miR-30a, hsa-miR-101, hsa-miR-497, hsa-miR-378, hsa-miR-214, hsa-miR-4324, hsa-miR-127-3p, hsa-miR-136, hsa-miR-1). Rock et al. observed that miR-21-5p and miR-31-5p expression were increased in invasive cSCC compared to normal tissue [48]. Olasz et al. discovered that miR-135b expression was upregulated in three cSCC cell lines [49]. Wang et al. demonstrated that microRNA-31 was highly expressed in cSCC and could regulate tumor biological processes [50]. Ma et al. indicated that miR-214 expression was low in both cSCC tissues and cells, and patients with higher miR-214 expression had a better prognosis [51]. Yamane et al. found that miR-214 was down-regulated in cSCC [52]. Shao et al. revealed that miR-30a-5p expression was reduced in SCL-1 and A431 cells [53]. Wei et al. also suggested that miR-497 was expressed lower in cSCC tissues and cells, and could promote the progression of cSCC [54]. The above results were consistent with our study. Then in order to further investigate circRNA-miRNA interactions. We intersected the miRNAs predicted by circRNAs and DEmiRNAs, and hsa-miR-136 and hsa-miR-766 were identified as the candidate miRNAs. Hsa-miR-136 was significantly down-regulated, and hsa-miR-766 was up-regulated in cSCC, which is consistent with our source data research [55]. Moreover, another study implied that miR-766 was upregulated in cSCC tissues and cells [56]. Sand et al. discovered that hsa-miR-766 was up-regulated in cSCC [55], which is consistent with our research.

A large amount of studies demonstrated that circRNAs could act as miRNA sponges and regulate miRNA-mediated gene expression, hence leading to the progression and development of tumors [57]. Chen et al. found that circ-ERBIN could contribute to the growth and metastasis of colorectal cancer by regulating miR-125a-5p and miR-138-5p [58]. Ma et al. discovered that hsa_circ_0004872 could inhibit gastric cancer progression by regulating miR-224/Smad4/ADAR [21]. To further evaluate the roles of DEcircRNAs in cSCC, the circRNA-microRNA-mRNA network was constructed. We found that the circRNA ceRNAs may provide new insight into the mechanism underlying cSCC. Gao et al. found that silencing circRNA_001937 might inhibit proliferation and induce apoptosis in cSCC by blocking sponging of the miRNA-597-3p/FOSL2 pathway [59]. Chen et al. revealed that circPVT1 might an important target for the treatment of cSCC [60]. Zhang et al. showed that hsa_circ_0070934 could regulate HOXB7 expression in cSCC by competitively sponging miR-1236-3p [39]. An et al. have found that circ_0070934 could promote the growth and invasion of cSCC cells by sponging miR-1238 and miR-1247-5p [36]. These studies indicated that the circRNA-related ceRNA network played an important role in the progression of cSCC. However, there is currently little research on it and our research has laid a good foundation for follow-up research.

GO and KEGG enrichment analyses were executed for the 36 genes in the network to study the biological functions of the circRNAs. Then we found the most enriched KEGG pathways were chemokine, RIG-I-like receptor signaling pathway, and microRNAs in cancer. Mittal et al. discovered that the CCR2/MCP-1 chemokine pathway played an important role in lung ade-

nocarcinoma [61]. Zhu et al. found that chemokine signaling pathways were involved in immune infiltration and the tumor microenvironment of sarcoma [62]. Next, the upregulated-hub genes of USP18, OAS3, ISG15, CXCL10 were identified in cSCC compared with normal tissues and PI3, RSAD2 were downregulated. In addition, the GO analysis showed that gens were most enriched in immune response in biological process. The previous study also showed the immune system played a significant role in cSCC progression [23, 63]. Then, 10 immune-related differentially expressed genes were obtained by overlapped with 36 differently expression genes in the ceRNA network and the lists of immune-related genes. The PPI network was constructed and the top hub genes were selected. CXCL10, ISG15 and IL7R were found to be upregulated in cSCC. PI3 and RSAD2 were downregulated. Moreover, Liu et al. also found that CXCL10 and ISG15 was a hub genes and might be potential targets for the diagnosis and therapy of patients with cSCC [64]. Toriseva et al. found that CXCL10 was associated with tumor progression in cSCC [65], which was consistent with our study.

In order to validate the above results and explore the biological functional implication of hub differentially expressed immune-related genes, the GO analysis found that they were mostly associated with immune response in the biological process and the most significant KEGG pathways were chemokine signaling pathway, microRNAs in cancer, and RIG-I-like receptor signaling pathway, which were consistent with the above results. These results suggest that circRNAs might compete binding to miRNAs to regulate the expression of immune-related genes to promote tumor progression. Liu et al. concluded that circRNAs could competitively bind PKR so that interfere the cellular immune signaling pathways [26]. Ng WL et al. revealed that macrophages could be activated under certain conditions and could produce circRNAs which could influence the immune functionality of macrophages [66]. Furthermore, circ-ANRIL might be involved in the apoptosis of macrophages and inhibit the proliferation of them [67]. It is clear that circRNAs could play a role in the activation and function of immune cells and influence tumor progression. Our study provides a good basis for further research on the immunomodulatory effects of circRNA on cSCC and related regulatory mechanisms.

Conclusion

Our study identified the DEcircRNAs, DEmiRNAs, DEmRNAs in cSCC and established the ceRNA network. Then, the immune-related genes were identified based on mRNAs in the ceRNA network and hub immune-related genes were validated by immunochemistry, which might act as potential diagnostic biomarkers, therapeutic targets, as well as new immune checkpoints for patients with cSCC.

Acknowledgements

The authors would like to thank GEO database (http://www.ncbi.nlm.nih.gov/geo/) and ImmPort (https://www.immport.org/shared/home) database for data collection. This research was supported by Sichuan Science and Technology Program (no, 2019YFS0109), China Postdoctoral Science Foundation (2019M663505), and Postdoctoral Interdisciplinary Innovation Foundation, Sichuan University (no, 004020-4153243).

Disclosure of conflict of interest

None.

Address correspondence to: Cheng Yi, Department of Medical Oncology, Cancer Center, West China Hospital, Sichuan University, 37 Guoxue Lane, Chengdu 610041, Sichuan, China. Tel: +86-18980601774; E-mail: yicheng6834@126.com

References

[1] Que SKT, Zwald FO and Schmults CD. Cutaneous squamous cell carcinoma: incidence, risk factors, diagnosis, and staging. J Am Acad Dermatol 2018; 78: 237-247.

[2] Reynolds K, Schlessinger D, Yanes A, Godinez-Puig V, Chen B, Kurta A, Cotseones J, Chiren S, Iyengar S, Ibrahim S, Kang B, Worley B, Behshad R, DeHoratius D, Denes P, Drucker A, Dzubow L, Etzkorn J, Harwood C, Kim J, Lawrence N, Lee E, Lissner G, Marghoob A, Matin R, Mattox A, Mittal B, Thomas J, Zhou X, Zloty D, Hughes B, Nottage M, Green A, Testori A, Argenziano G, Longo C, Zalaudek I, Lebbe C, Malvehy J, Saiag P, Cernea S, Schmitt J, Kirkham J, Poon E, Sobanko J, Cartee T, Maher I and Alam M. Development of a core outcome set for cutaneous squamous cell carcinoma trials: identification of core domains and outcomes. Br J Dermatol 2021; 184: 1113-1122.

[3] Chong K, Daud A, Ortiz-Urda S and Arron ST; UCSF High Risk Skin Cancer Program. Cutting

edge in medical management of cutaneous oncology. Semin Cutan Med Surg 2012; 31: 140-149.
[4] Kauvar AN, Arpey CJ, Hruza G, Olbricht SM, Bennett R and Mahmoud BH. Consensus for nonmelanoma skin cancer treatment, part II: squamous cell carcinoma, including a cost analysis of treatment methods. Dermatol Surg 2015; 41: 1214-1240.
[5] Eversman A, Tracey EH, Michalik D, Rodriguez M, Varra V, Briskin IN, Vidimos AT and Pobletе-Lopez CM. Moderate differentiation is a risk factor for extensive subclinical spread of cutaneous squamous cell carcinoma. J Am Acad Dermatol 2020; [Epub ahead of print].
[6] Brunner M, Veness MJ, Ch'ng S, Elliott M and Clark JR. Distant metastases from cutaneous squamous cell carcinoma--analysis of AJCC stage IV. Head Neck 2013; 35: 72-75.
[7] Chen LL. The expanding regulatory mechanisms and cellular functions of circular RNAs. Nat Rev Mol Cell Biol 2020; 21: 475-490.
[8] Kristensen LS, Andersen MS, Stagsted LVW, Ebbesen KK, Hansen TB and Kjems J. The biogenesis, biology and characterization of circular RNAs. Nat Rev Genet 2019; 20: 675-691.
[9] Chen LL. The biogenesis and emerging roles of circular RNAs. Nat Rev Mol Cell Biol 2016; 17: 205-211.
[10] Guarnerio J, Zhang Y, Cheloni G, Panella R, Mae Katon J, Simpson M, Matsumoto A, Papa A, Loretelli C, Petri A, Kauppinen S, Garbutt C, Nielsen GP, Deshpande V, Castillo-Martin M, Cordon-Cardo C, Dimitrios S, Clohessy JG, Batish M and Pandolfi PP. Intragenic antagonistic roles of protein and circRNA in tumorigenesis. Cell Res 2019; 29: 628-640.
[11] Vo JN, Cieslik M, Zhang Y, Shukla S, Xiao L, Zhang Y, Wu YM, Dhanasekaran SM, Engelke CG, Cao X, Robinson DR, Nesvizhskii AI and Chinnaiyan AM. The landscape of circular RNA in cancer. Cell 2019; 176: 869-881, e13.
[12] Lu D and Thum T. RNA-based diagnostic and therapeutic strategies for cardiovascular disease. Nat Rev Cardiol 2019; 16: 661-674.
[13] Aufiero S, Reckman YJ, Pinto YM and Creemers EE. Circular RNAs open a new chapter in cardiovascular biology. Nat Rev Cardiol 2019; 16: 503-514.
[14] Shan K, Liu C, Liu BH, Chen X, Dong R, Liu X, Zhang YY, Liu B, Zhang SJ, Wang JJ, Zhang SH, Wu JH, Zhao C and Yan B. Circular noncoding RNA HIPK3 mediates retinal vascular dysfunction in diabetes mellitus. Circulation 2017; 136: 1629-1642.
[15] Xu H, Liu Y, Cheng P, Wang C, Liu Y, Zhou W, Xu Y and Ji G. CircRNA_0000392 promotes colorectal cancer progression through the miR-193a-5p/PIK3R3/AKT axis. J Exp Clin Cancer Res 2020; 39: 283.
[16] Pan Z, Cai J, Lin J, Zhou H, Peng J, Liang J, Xia L, Yin Q, Zou B, Zheng J, Qiao L and Zhang L. A novel protein encoded by circFNDC3B inhibits tumor progression and EMT through regulating Snail in colon cancer. Mol Cancer 2020; 19: 71.
[17] Bezzi M, Guarnerio J and Pandolfi PP. A circular twist on microRNA regulation. Cell Res 2017; 27: 1401-1402.
[18] Xu H, Wang C, Song H, Xu Y and Ji G. RNA-Seq profiling of circular RNAs in human colorectal cancer liver metastasis and the potential biomarkers. Mol Cancer 2019; 18: 8.
[19] Lu C, Shi X, Wang AY, Tao Y, Wang Z, Huang C, Qiao Y, Hu H and Liu L. RNA-Seq profiling of circular RNAs in human laryngeal squamous cell carcinomas. Mol Cancer 2018; 17: 86.
[20] Li J, Sun D, Pu W, Wang J and Peng Y. Circular RNAs in cancer: biogenesis, function, and clinical significance. Trends Cancer 2020; 6: 319-336.
[21] Ma C, Wang X, Yang F, Zang Y, Liu J, Wang X, Xu X, Li W, Jia J and Liu Z. Circular RNA hsa_circ_0004872 inhibits gastric cancer progression via the miR-224/Smad4/ADAR1 successive regulatory circuit. Mol Cancer 2020; 19: 157.
[22] Zhang PF, Pei X, Li KS, Jin LN, Wang F, Wu J and Zhang XM. Circular RNA circFGFR1 promotes progression and anti-PD-1 resistance by sponging miR-381-3p in non-small cell lung cancer cells. Mol Cancer 2019; 18: 179.
[23] Borradori L, Sutton B, Shayesteh P and Daniels GA. Rescue therapy with anti-programmed cell death protein 1 inhibitors of advanced cutaneous squamous cell carcinoma and basosquamous carcinoma: preliminary experience in five cases. Br J Dermatol 2016; 175: 1382-1386.
[24] In GK, Vaidya P, Filkins A, Hermel DJ, King KG, Ragab O, Tseng WW, Swanson M, Kokot N, Lang JE, Menendez L, DeClerck B, Kim G, Hu JC, Terando A, Jadvar H, Ricker C, Miller KA, Peng DH and Wysong A. PD-1 inhibition therapy for advanced cutaneous squamous cell carcinoma: a retrospective analysis from the University of Southern California. J Cancer Res Clin Oncol 2021; 147: 1803-1811.
[25] Wilusz JE. Circle the wagons: circular RNAs control innate immunity. Cell 2019; 177: 797-799.
[26] Liu CX, Li X, Nan F, Jiang S, Gao X, Guo SK, Xue W, Cui Y, Dong K, Ding H, Qu B, Zhou Z, Shen N, Yang L and Chen LL. Structure and degradation of circular RNAs regulate PKR activation in innate immunity. Cell 2019; 177: 865-880, e21.
[27] Wei CY, Zhu MX, Lu NH, Liu JQ, Yang YW, Zhang Y, Shi YD, Feng ZH, Li JX, Qi FZ and Gu JY. Circular RNA circ_0020710 drives tumor pro-

gression and immune evasion by regulating the miR-370-3p/CXCL12 axis in melanoma. Mol Cancer 2020; 19: 84.
[28] Hong W, Xue M, Jiang J, Zhang Y and Gao X. Circular RNA circ-CPA4/ let-7 miRNA/PD-L1 axis regulates cell growth, stemness, drug resistance and immune evasion in non-small cell lung cancer (NSCLC). J Exp Clin Cancer Res 2020; 39: 149.
[29] Li L, Zhang Q and Lian K. Circular RNA circ_0000284 plays an oncogenic role in the progression of non-small cell lung cancer through the miR-377-3p-mediated PD-L1 promotion. Cancer Cell Int 2020; 20: 247.
[30] Glažar P, Papavasileiou P and Rajewsky N. circBase: a database for circular RNAs. RNA 2014; 20: 1666-1670.
[31] Goodall GJ and Wickramasinghe VO. RNA in cancer. Nat Rev Cancer 2021; 21: 22-36
[32] Guarnerio J, Bezzi M, Jeong JC, Paffenholz SV, Berry K, Naldini MM, Lo-Coco F, Tay Y, Beck AH and Pandolfi PP. Oncogenic role of fusion-circRNAs derived from cancer-associated chromosomal translocations. Cell 2016; 165: 289-302.
[33] Liu Y, Li Z, Zhang M, Zhou H, Wu X, Zhong J, Xiao F, Huang N, Yang X, Zeng R, Yang L, Xia Z and Zhang N. Rolling-translated EGFR variants sustain EGFR signaling and promote glioblastoma tumorigenicity. Neuro Oncol 2021; 23: 743-756.
[34] Kashyap MP, Sinha R, Mukhtar MS and Athar M. Epigenetic regulation in the pathogenesis of non-melanoma skin cancer. Semin Cancer Biol 2020; [Epub ahead of print].
[35] Sand M, Bechara FG, Gambichler T, Sand D, Bromba M, Hahn SA, Stockfleth E and Hessam S. Circular RNA expression in cutaneous squamous cell carcinoma. J Dermatol Sci 2016; 83: 210-218.
[36] An X, Liu X, Ma G and Li C. Upregulated circular RNA circ_0070934 facilitates cutaneous squamous cell carcinoma cell growth and invasion by sponging miR-1238 and miR-1247-5p. Biochem Biophys Res Commun 2019; 513: 380-385.
[37] Zhou L, Wang Y, Zhou M, Zhang Y, Wang P, Li X, Yang J, Wang H and Ding Z. HOXA9 inhibits HIF-1α-mediated glycolysis through interacting with CRIP2 to repress cutaneous squamous cell carcinoma development. Nat Commun 2018; 9: 1480.
[38] An X, Xu G, Yang L, Wang Y, Li Y, McHepange UO, Shen G, Tu Y and Tao J. Expression of hypoxia-inducible factor-1α, vascular endothelial growth factor and prolyl hydroxylase domain protein 2 in cutaneous squamous cell carcinoma and precursor lesions and their relationship with histological stages and clinical features. J Dermatol 2014; 41: 76-83.
[39] Zhang DW, Wu HY, Zhu CR and Wu DD. CircRNA hsa_circ_0070934 functions as a competitive endogenous RNA to regulate HOXB7 expression by sponging miR-1236-3p in cutaneous squamous cell carcinoma. Int J Oncol 2020; 57: 478-487.
[40] Zhang T, Jing B, Bai Y, Zhang Y and Yu H. Circular RNA circTMEM45A acts as the sponge of MicroRNA-665 to promote hepatocellular carcinoma progression. Mol Ther Nucleic Acids 2020; 22: 285-297.
[41] Ding B, Fan W and Lou W. In Vitrohsa_circ_0001955 enhances proliferation, migration, and invasion of HCC cells through miR-145-5p/NRAS axis. Mol Ther Nucleic Acids 2020; 22: 445-455.
[42] Ding B, Yao M, Fan W and Lou W. Whole-transcriptome analysis reveals a potential hsa_circ_0001955/hsa_circ_0000977-mediated miRNA-mRNA regulatory sub-network in colorectal cancer. Aging (Albany BY) 2020; 12: 5259-5279.
[43] Murray M and Coleman N. MicroRNA dysregulation in malignant germ cell tumors: more than a biomarker? J Clin Oncol 2019; 37: 1432-1435.
[44] Rupaimoole R and Slack FJ. MicroRNA therapeutics: towards a new era for the management of cancer and other diseases. Nat Rev Drug Discov 2017; 16: 203-222.
[45] Xu J, Zhang Y, Huang Y, Dong X, Xiang Z, Zou J, Wu L and Lu W. circEYA1 functions as a sponge of miR-582-3p to suppress cervical adenocarcinoma tumorigenesis via upregulating CXCL14. Mol Ther Nucleic Acids 2020; 22: 1176-1190.
[46] Hao L, Rong W, Bai L, Cui H, Zhang S, Li Y, Chen D and Meng X. Upregulated circular RNA circ_0007534 indicates an unfavorable prognosis in pancreatic ductal adenocarcinoma and regulates cell proliferation, apoptosis, and invasion by sponging miR-625 and miR-892b. J Cell Biochem 2019; 120: 3780-3789.
[47] Niu Q, Dong Z, Liang M, Luo Y, Lin H, Lin M, Zhong X, Yao W, Weng J and Zhou X. Circular RNA hsa_circ_0001829 promotes gastric cancer progression through miR-155-5p/SMAD2 axis. J Exp Clin Cancer Res 2020; 39: 280.
[48] Rock AN, Fisher MD, Amborski G, Allain DC, Klee V, Peters SB, Kang S and Toland AE. MicroRNA expression profiling of cutaneous squamous cell carcinomas arising in different sites. Otolaryngol Head Neck Surg 2020; 163: 538-545.
[49] Olasz EB, Seline LN, Schock AM, Duncan NE, Lopez A, Lazar J, Flister MJ, Lu Y, Liu P, Sokumbi O, Harwood CA, Proby CM, Neuburg M and Lazarova Z. MicroRNA-135b regulates leucine zipper tumor suppressor 1 in cutaneous squamous cell carcinoma. PLoS One 2015; 10: e0125412.

[50] Wang A, Landén NX, Meisgen F, Lohcharoenkal W, Ståhle M, Sonkoly E and Pivarcsi A. MicroRNA-31 is overexpressed in cutaneous squamous cell carcinoma and regulates cell motility and colony formation ability of tumor cells. PLoS One 2014; 9: e103206.
[51] Ma X, Wu D, Zhang X, Shao X and Hu G. microRNA-214 prevents traits of cutaneous squamous cell carcinoma via VEGFA and Bcl-2. Technol Cancer Res Treat 2020; 19: 1533033820980098.
[52] Yamane K, Jinnin M, Etoh T, Kobayashi Y, Shimozono N, Fukushima S, Masuguchi S, Maruo K, Inoue Y, Ishihara T, Aoi J, Oike Y and Ihn H. Down-regulation of miR-124/-214 in cutaneous squamous cell carcinoma mediates abnormal cell proliferation via the induction of ERK. J Mol Med (Berl) 2013; 91: 69-81.
[53] Shao J, Liang J and Zhong S. miR-30a-5p modulates traits of cutaneous squamous cell carcinoma (cSCC) via forkhead box protein G1 (FOXG1). Neoplasma 2019; 66: 908-917.
[54] Wei XH, Gu XL, Zhou XT, Ma MM and Lou CX. miR-497 promotes the progression of cutaneous squamous cell carcinoma through FAM-114A2. Eur Rev Med Pharmacol Sci 2018; 22: 7348-7355.
[55] Sand M, Skrygan M, Georgas D, Sand D, Hahn SA, Gambichler T, Altmeyer P and Bechara FG. Microarray analysis of microRNA expression in cutaneous squamous cell carcinoma. J Dermatol Sci 2012; 68: 119-126.
[56] Liu P, Shi L, Ding Y, Luan J, Shan X, Li Q and Zhang S. MicroRNA-766 promotes the proliferation, migration and invasion, and inhibits the apoptosis of cutaneous squamous cell carcinoma cells by targeting PDCD5. Onco Targets Ther 2020; 13: 4099-4110.
[57] Kristensen LS, Hansen TB, Venø MT and Kjems J. Circular RNAs in cancer: opportunities and challenges in the field. Oncogene 2018; 37: 555-565.
[58] Chen L, Wang L, Ren Y, Pang Z, Liu Y, Sun X, Tu J, Zhi Z, Qin Y, Sun L and Li J. The circular RNA circ-ERBIN promotes growth and metastasis of colorectal cancer by miR-125a-5p and miR-138-5p/4EBP-1 mediated cap-independent HIF-1α translation. Mol Cancer 2020; 19: 164.
[59] Gao L, Jin HJ, Zhang D and Lin Q. Silencing circRNA_001937 may inhibit cutaneous squamous cell carcinoma proliferation and induce apoptosis by preventing the sponging of the miRNA-597-3p/FOSL2 pathway. Int J Mol Med 2020; 46: 1653-1660.
[60] Chen S, Ding J, Wang Y, Lu T, Wang L, Gao X, Chen H, Qu L and He C. RNA-Seq profiling of circular RNAs and the oncogenic role of circPVT1 in cutaneous squamous cell carcinoma. Onco Targets Ther 2020; 13: 6777-6788.
[61] Mittal P, Wang L, Akimova T, Leach CA, Clemente JC, Sender MR, Chen Y, Turunen BJ and Hancock WW. The CCR2/MCP-1 chemokine pathway and lung adenocarcinoma. Cancers 2020; 12: 3723.
[62] Zhu N and Hou J. Assessing immune infiltration and the tumor microenvironment for the diagnosis and prognosis of sarcoma. Cancer Cell Int 2020; 20: 577.
[63] Fujimura T, Kambayashi Y, Tono H, Lyu C, Ohuchi K, Hashimoto A and Aiba S. Successful treatment of unresectable recurrent cutaneous squamous cell carcinoma of the scalp with meningeal invasion with nivolumab monotherapy. Dermatol Ther 2020; 33: e13672.
[64] Liu H, Chen D, Liu P, Xu S, Lin X and Zeng R. Secondary analysis of existing microarray data reveals potential gene drivers of cutaneous squamous cell carcinoma. J Cell Physiol 2019; [Epub ahead of print].
[65] Toriseva M, Ala-aho R, Peltonen S, Peltonen J, Grénman R and Kähäri VM. Keratinocyte growth factor induces gene expression signature associated with suppression of malignant phenotype of cutaneous squamous carcinoma cells. PloS One 2012; 7: e33041.
[66] Ng WL, Marinov GK, Liau ES, Lam YL, Lim YY and Ea CK. Inducible RasGEF1B circular RNA is a positive regulator of ICAM-1 in the TLR4/LPS pathway. RNA Biol 2016; 13: 861-871.
[67] Holdt LM, Stahringer A, Sass K, Pichler G, Kulak NA, Wilfert W, Kohlmaier A, Herbst A, Northoff BH, Nicolaou A, Gäbel G, Beutner F, Scholz M, Thiery J, Musunuru K, Krohn K, Mann M and Teupser D. Circular non-coding RNA ANRIL modulates ribosomal RNA maturation and atherosclerosis in humans. Nat Commun 2016; 7: 12429.

Supplementary Table 1. Basic information of the 5 microarray datasets from GEO

Data source	Organism	Platform	Contributor(s)	Experiment type	Update year	Region	Sample size	RNA type
GSE74758	Homo sapiens	GPL19978 Agilent-069978 Arraystar Human CircRNA microarray V1	Sand M	Non-coding RNA profiling by array	2016	Germany	cSCC (n=3) and non-lesional skin (n=3)	circRNA
GSE34536	Homo sapiens	GPL15019 Agilent-031181 Unrestricted_Human_miRNA_V16.0_Microarray 030840 (miRBase release 14.0 miRNA ID version)	Sand M	Non-coding RNA profiling by array	2013	Germany	cSCC (n=7) and adjacent healthy skin (n=7)	miRNA
GSE45164	Homo sapiens	GPL571 [HG-U133A_2] Affymetrix Human Genome U133A 2.0 Array	Brooks Y	Expression profiling by array	2018	Italy	cSCC (n=10) and normal human epidermis controls (n=3)	mRNA
GSE66359	Homo sapiens	GPL570 [HG-U133_Plus_2] Affymetrix Human Genome U133 Plus 2.0 Array	Farshchian M	Expression profiling by array	2019	Finland	cSCC (n=8) and normal human epidermal keratinocytes (n=5)	mRNA
GSE42677	Homo sapiens	GPL571 [HG-U133A_2] Affymetrix Human Genome U133A 2.0 Array	Mitsui H	Expression profiling by array	2019	USA	cSCC (n=10) and normal skin epidermal cells (n=10)	mRNA

Supplementary Table 2. The differentially expressed circRNAs

circBase ID	logFC	*P* Value	regulation	source	position	best transcript	gene names
hsa_circ_0068631	2.984716944	0.008509	up	circBase	chr3:195802029-195803993	NM_003234	TFRC
hsa_circ_0070933	2.933784833	0.000342	up	circBase	chr4:128995614-128996148	NM_018078	LARP1B
hsa_circ_0067772	2.601642222	0.00443	up	circBase	chr3:155547476-155560408	NM_004733	SLC33A1
hsa_circ_0003528	2.59531925	0.004158	up	circBase	chr5:134032815-134044578	NM_021982	SEC24A
hsa_circ_0070934	2.589680778	0.00126	up	circBase	chr4:128995614-129012667	NM_018078	LARP1B
hsa_circ_0001955	2.564198778	0.001089	up	circBase	chr15:64495280-64508912	NM_022048	CSNK1G1
hsa_circ_0000851	2.550416	0.025832	up	circBase	chr18:52926327-52926446	NM_001243234	TCF4
hsa_circ_0009065	2.532981278	0.001553	up	circBase	chr16:14738130-14738466	NM_016561	BFAR
hsa_circ_0032704	2.528467167	0.003264	up	circBase	chr14:76173360-76187046	NM_015072	TTLL5
hsa_circ_0035381	2.497717056	0.001805	up	circBase	chr15:55621921-55634000	NM_004855	PIGB
hsa_circ_0088494	2.444748778	0.005248	up	circBase	chr9:127083737-127089724	NM_001145001	NEK6
hsa_circ_0074817	2.427390778	0.003119	up	circBase	chr5:158204420-158223486	NM_024007	EBF1
hsa_circ_0053932	2.363159389	0.002089	up	circBase	chr2:33525517-33525640	NM_206943	LTBP1
hsa_circ_0001402	2.320825889	3.73E-05	up	circBase	chr4:38091552-38104778	NM_015173	TBC1D1
hsa_circ_0079375	2.315624778	0.001288	up	circBase	chr7:6618131-6624891	NM_018106	ZDHHC4
hsa_circ_0086563	2.303683694	0.012498	up	circBase	chr9:20907148-20926416	NM_017794	KIAA1797
hsa_circ_0002069	2.248800056	0.000931	up	circBase	chr17:46189392-46190763	NM_152244	SNX11
hsa_circ_0004136	2.211108778	0.003149	up	circBase	chr6:73713630-73751785	NM_001160133	KCNQ5
hsa_circ_0079480	2.20990025	0.013876	up	circBase	chr7:16298014-16317851	NM_001101426	ISPD
hsa_circ_0007146	2.198776	0.002319	up	circBase	chr16:5077135-5078186	NM_016256	NAGPA
hsa_circ_0078155	2.178423306	0.004903	up	circBase	chr6:147527106-147655358	NM_001127715	STXBP5
hsa_circ_0000228	2.161570722	0.003073	up	circBase	chr10:31661946-31676195	NM_030751	ZEB1
hsa_circ_0000844	2.1496425	0.027974	up	circBase	chr18:42269709-42269921	NM_001130110	SETBP1
hsa_circ_0007976	2.1242365	0.000584	up	circBase	chr14:62188226-62188541	NM_001530	HIF1A
hsa_circ_0034972	2.086038778	0.03649	up	circBase	chr15:43692241-43694048	NM_014444	TUBGCP4
hsa_circ_0004365	2.072752056	0.000439	up	circBase	chr7:80418621-80440017	NM_006379	SEMA3C
hsa_circ_0008274	2.061942667	0.003318	up	circBase	chr13:96485180-96489456	NM_020121	UGGT2
hsa_circ_0004795	2.012424444	0.023797	up	circBase	chr22:38948670-38964294	NM_007068	DMC1
hsa_circ_0022392	-5.562538167	7.57E-08	down	circBase	chr11:61630443-61631258	NM_004265	FADS2
hsa_circ_0022383	-5.410590778	3.68E-07	down	circBase	chr11:61605249-61615756	NM_004265	FADS2
hsa_circ_0005085	-4.348301556	2.05E-05	down	circBase	chr2:9419445-9437574	NM_003887	ASAP2
hsa_circ_0046449	-3.714428278	0.00126	down	circBase	chr17:80714040-80758872	NM_005993	TBCD
hsa_circ_0072279	-3.601349444	0.000606	down	circBase	chr5:37352838-37358253	NM_153485	NUP155
hsa_circ_0000375	-3.501067111	0.000994	down	circBase	chr12:6657590-6657991	NM_080730	IFFO1
hsa_circ_0075410	-3.401683889	0.000805	down	circBase	chr6:304627-311962	NM_020185	DUSP22
hsa_circ_0046464	-2.640867	0.002184	down	circBase	chr17:80721840-80758872	NM_005993	TBCD
hsa_circ_0001525	-2.53182	0.002661	down	circBase	chr5:131761180-131761386	NR_045116	C5orf56
hsa_circ_0002456	-2.497622889	0.000759	down	circBase	chr10:128923737-128926028	NM_001380	DOCK1
hsa_circ_0072389	-2.383522389	0.001839	down	circBase	chr5:43294157-43299077	NM_001098272	HMGCS1
hsa_circ_0006470	-2.356841778	0.005208	down	circBase	chr1:12061457-12062160	NM_014874	MFN2
hsa_circ_0007928	-2.347996556	9.70E-05	down	circBase	chr4:52729602-52752804	NM_001040402	DCUN1D4
hsa_circ_0072386	-2.265338389	0.006446	down	circBase	chr5:43292575-43299077	NM_001098272	HMGCS1
hsa_circ_0001410	-2.216346056	2.01E-05	down	circBase	chr4:52729602-52744020	NM_015115	DCUN1D4
hsa_circ_0000977	-2.213772389	0.004045	down	circBase	chr2:10784445-10808849	NM_024894	NOL10
hsa_circ_0063331	-2.188443167	0.002135	down	circBase	chr22:38894089-38897285	NM_001098504	DDX17
hsa_circ_0000026	-2.141387278	0.002812	down	circBase	chr1:21377358-21437876	NM_001198803	EIF4G3
hsa_circ_0002404	-2.129998278	0.007976	down	circBase	chr17:35603741-35609962	NM_198839	ACACA
hsa_circ_0002733	-2.115744722	0.001967	down	circBase	chr1:16046228-16047883	NM_015164	PLEKHM2
hsa_circ_0001549	-2.094346222	0.001003	down	circBase	chr5:159664587-159664757	NM_001040442	FABP6
hsa_circ_0076251	-2.090398667	0.000211	down	circBase	chr6:38050167-38084515	NM_021943	ZFAND3
hsa_circ_0031027	-2.065290056	0.016144	down	circBase	chr13:114164552-114193822	NM_017905	TMCO3
hsa_circ_0015449	-2.032155889	6.92E-05	down	circBase	chr1:179311248-179312770	NM_003101	SOAT1
hsa_circ_0089252	-2.029348389	6.30E-05	down	circBase	chr9:134514021-134526336	NM_198679	RAPGEF1
hsa_circ_0005571	-2.026883556	0.001749	down	circBase	chr19:18285849-18286507	NM_006332	IFI30

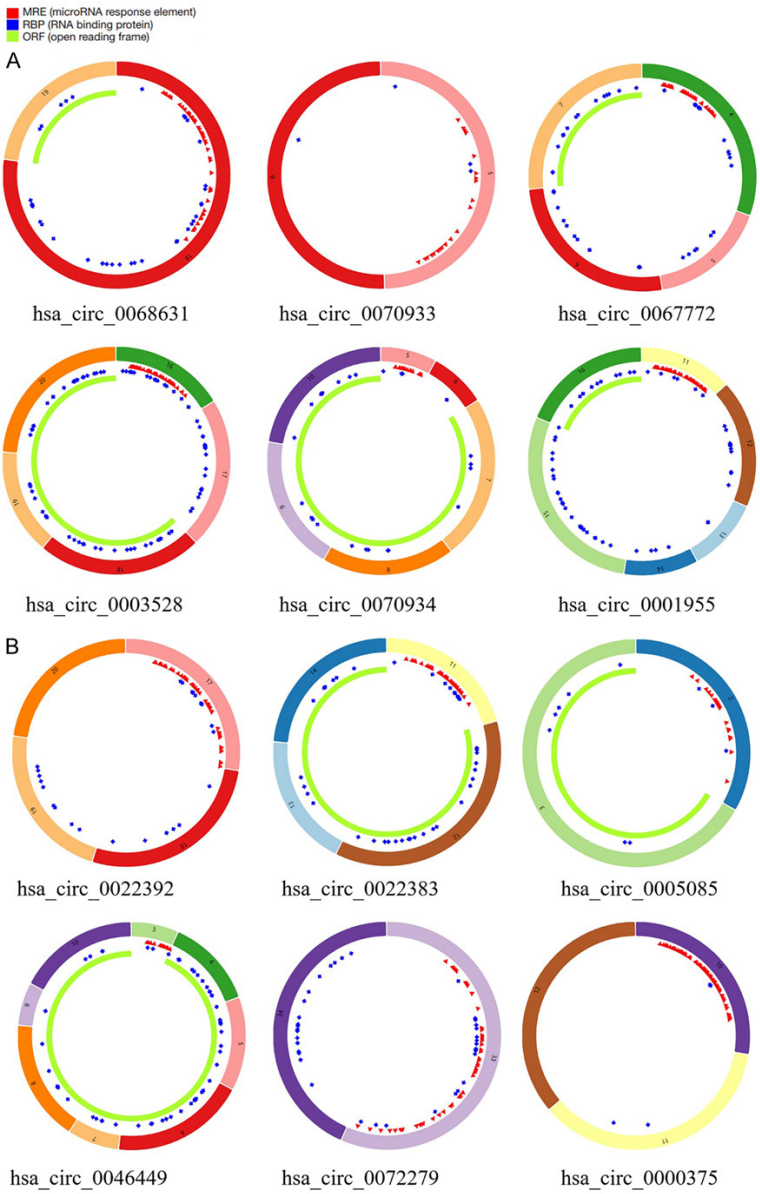

Supplementary Figure 1. Structural graphs of the top 12 circRNAs. A. Top 6 up-regulated circRNAs; B. Top 6 down-regulated circRNAs. Red spots represent miRNA response elements, blue spots represent RNA binding protein, and green curves represent the open reading frame.

Supplementary Table 3. 10 immune-related differentially expressed genes

Gene symbol	Description	Chromosome	Map location
PI3	peptidase inhibitor 3, skin-derived	20	20q13.12
CXCL10	chemokine (C-X-C motif) ligand 10	4	4q21
ISG15	ISG15 ubiquitin-like modifier	1	1p36.33
BST2	bone marrow stromal cell antigen 2	19	19p13.1
IL7R	interleukin 7 receptor	5	5p13
HDAC1	histone deacetylase 1	1	1p34
RSAD2	radical S-adenosyl methionine domain containing 2	2	2p25.2
LYN	LYN proto-oncogene, Src family tyrosine kinase	8	8q13
TNC	tenascin C	9	9q33
SHC1	SHC (Src homology 2 domain containing) transforming protein 1	1	1q21